A tool for designing digital filters for the Hankel and Fourier transforms in potential, diffusive, and wavefield modeling

Werthmüller, Dieter; Key, Kerry; Slob, Evert C.

DOI
10.1190/GEO2018-0069.1

Publication date
2019

Document Version
Final published version

Published in
Geophysics

GEOPHYSICS, VOL. 84, NO. 2 (MARCH-APRIL 2019); P. F47–F56, 11 FIGS.
10.1190/GEO2018-0069.1

A tool for designing digital filters for the Hankel and Fourier transforms in potential, diffusive, and wavefield modeling

Dieter Werthmüller[1], Kerry Key[2], and Evert C. Slob[3]

ABSTRACT

The open-source code `fdesign` makes it possible to design digital linear filters for the Hankel and Fourier transforms used in potential, diffusive, and wavefield modeling. Digital filters can be derived for any electromagnetic (EM) method, such as methods in the diffusive limits (direct current, controlled-source EM [CSEM]) as well as methods using higher frequency content (ground-penetrating radar [GPR], acoustic and elastic wavefields). The direct matrix inversion method is used for the derivation of the filter values, and a brute-force minimization search is carried out over the defined spacing and shifting values of the filter basis. Included or user-provided theoretical transform pairs are used for the inversion. Alternatively, one can provide layered subsurface models that will be computed with a precise quadrature method using the EM modeler `empymod` to generate numerical transform pairs. The comparison of the presented 201 pt filter with previously presented filters indicates that it performs better for some standard CSEM cases. The derivation of a longer 2001 pt filter for a GPR example with a 250 MHz center frequency proves that the filter method works not only for diffusive EM fields but also for wave phenomena. The presented algorithm provides a tool to create problem specific digital filters. Such purpose-built filters can be made shorter and can speed up consecutive potential, diffusive, and wavefield inversions.

INTRODUCTION

In his Ph.D. thesis, Ghosh (1970) proposes a linear filter method for the numerical evaluation of Hankel transforms that subsequently revolutionized the computation of electromagnetic (EM) responses in the field of geophysical exploration. If you use a code that calculates EM responses in the wavenumber-frequency domain and transforms them to the space-frequency domain, chances are high that it uses the digital linear filter (DLF) method. Most practical 1D EM modeling codes rely on the DLF method for rapid computations; these codes are not only used for stand-alone simulations of EM fields in layered 1D media, but they are also commonly embedded within 3D modeling codes for computing the primary fields in scattered-field formulations or for the background fields required by integral equation methods. Thus, the DLF method is an important component of many commonly used modeling codes for EM geophysical data.

Ghosh (1971a) states that the DLF idea is based on suggestions made four decades earlier by Slichter (1933) and Pekeris (1940), in that "the kernel function is dependent only on the layer parameters, and an expression relating it to the field measurements can be obtained by mathematical processes." However, until the introduction of DLF, these suggestions found no widespread use, likely because of the missing computer power to calculate the filter coefficients. He further states that credit goes to Koefoed (1968, 1970), who retook the task of direct interpretational methods with the introduction of raised kernel functions. DLF is, as such, an improvement of that approach, providing a faster and simpler method.

The DLF technique is sometimes referred to as the fast Hankel transform (FHT), popular because of the similarity of the name to the well-

Peer-reviewed code related to this article can be found at http://software.seg.org/2019/0003.
Manuscript received by the Editor 25 January 2018; revised manuscript received 19 June 2018; published ahead of production 03 December 2018; published online 05 March 2019.
[1]Formerly Instituto Mexicano del Petróleo, Eje Central Lázaro Cárdenas Norte 152, Col. San Bartolo Atepehuacan C.P. 07730, Ciudad de México, México; presently TU Delft, Building 23, Stevinweg 1/PO-box 5048, CN Delft 2628, The Netherlands. E-mail: d.werthmuller@tudelft.nl.
[2]Columbia University, Lamont-Doherty Earth Observatory, 61 Route 9W, Palisades, New York 10964-8000, USA. E-mail: kkey@ldeo.columbia.edu.
[3]TU Delft, Building 23, Stevinweg 1/PO-box 5048, CN Delft 2628, The Netherlands. E-mail: e.c.slob@tudelft.nl.

known fast Fourier transform (FFT), although the algorithms for these techniques are completely different. The FHT name was likely inspired by the title of a paper by Johansen and Sørensen (1979). However, the name FHT can be misleading because it has Hankel in the name, whereas the DLF approach can more generally be applied to other linear transforms, for example, Fourier sine and cosine transforms.

The introduction of linear filters to EM geophysics, in parallel with rising computational power, initiated a wealth of investigations, leading to the development of computer programs that extended and improved the DLF method, and to numerous publications. These publications fall broadly into one or several of three categories: (1) new applications that extend the use of DLF to other EM measurement techniques, (2) filter improvements that provide either new filters or improved methods for the determination of filter coefficients, and (3) computational tools that compute EM responses using DLF techniques. Here, we briefly review the most relevant publications, without claiming completeness.

New applications

Ghosh uses the method originally for the computation of type curves for Schlumberger and Wenner resistivity soundings: Ghosh (1971a) derives a resistivity model from given Schlumberger or Wenner sounding curves, and Ghosh (1971b) provides filters for the inverse operation, deriving resistivity sounding curves from a given resistivity model. The method was next applied to EM soundings with horizontal and perpendicular coils (Koefoed et al., 1972), to vertical coplanar coil systems (Verma and Koefoed, 1973), to dipoles and other two-electrode systems (Das and Ghosh, 1974; Das et al., 1974; Das and Verma, 1980; Sørensen and Christensen, 1994), and to vertical dikes, hence vertical instead of horizontal layers (Niwas, 1975). The first filters were specific to a particular resistivity sounding type and its transform; later publications used the method to get one type curve from another type curve (Kumar and Das, 1977, 1978), or they generalized the method to be applicable to a wider set of problems (Davis et al., 1980; Das and Verma, 1981b; Das, 1984; O'Neill and Merrick, 1984). Eventually, it passed from pure layered modeling to primary-secondary field formulations for 3D problems, in which DLF is used to compute the spatial Fourier-Hankel transforms in a horizontally layered background medium and to compute transient responses from frequency-domain computations (Das and Verma, 1981a, 1982; Anderson, 1984; Newman et al., 1986; Kruglyakov and Bloshanskaya, 2017). Other publications delved into the theory of the method, analyzing the oscillating behavior of the filters and trying to estimate the error of DLF (Koefoed, 1972, 1976; Johansen and Sørensen, 1979; Christensen, 1990).

Filter improvements

Ghosh (1970) derives the filter coefficients in the spectral domain by dividing the output spectrum by the input spectrum followed by an inverse Fourier transform. Improvements to the determination of filter coefficients were provided by O'Neill (1975), Nyman and Landisman (1977), Das (1982), or specifically for the Fourier transform by Nissen and Enmark (1986). A direct integration method was used by Bichara and Lakshmanan (1976) and Bernabini and Cardarelli (1978). Koefoed and Dirks (1979) propose a Wiener-Hopf least-squares method that was further improved by many authors (Guptasarma, 1982; Murakami and Uchida, 1982; Guptasarma and Singh, 1997). Kong (2007) proposes a direct matrix inversion method to solve the convolution equation, which requires only the input and output sample values. To evaluate the filter's effectiveness, he defines a good filter as one that recovers small or weak diffusive EM fields. This method was also used by Key (2009, 2012) to create a suite of filters accurate for marine EM data. Most works have published filters for the Hankel transform with J_0 and J_1 Bessel functions (or $J_{-1/2}$, $J_{1/2}$ if applied to the Fourier sine/cosine transform), as all higher Bessel functions can be rewritten, via recurrence relations, using only these two. Mohsen and Hashish (1994) is one of the rare cases that provide J_2 filter weights.

Computational tools

The most well-known codes are likely Anderson's freely available ones. Anderson (1973) extends the method to transient responses, applying DLF not only to the Hankel transform but also to the Fourier transform. A transient signal can therefore be obtained by twice applying a digital filter to the wavenumber-frequency domain calculation. Anderson (1975, 1979) presents improved filters for the Fourier and Hankel transforms, introducing measures to significantly speed up the calculation, such as the lagged convolution or using the same abscissae for J_0 and J_1. Anderson (1982) and the included 801 pt filter became the de facto industry standard, to which subsequent filters were compared. Anderson (1989) presents a hybrid solution that uses either the DLF or a much slower but highly accurate adaptive-quadrature approach, which can also be used to measure the accuracy of the DLF. Key (2012) presents codes for comparing the DLF approach with a speed optimized quadrature method called quadrature-with-extrapolation (QWE); despite its optimizations, QWE is still not as fast as DLF, but it remains valuable as an independent tool for testing the accuracy of particular filters for the DLF method. Other examples include the codes by Johansen (1975), an interactive system for interpretation of resistivity soundings, and a tool to calculate filter coefficients by Christensen (1990). The latter is available upon request and was used, for instance, in all the open-source modeling and inversion routines of CSIRO in the Amira Project 223 (Raiche et al., 2007).

All of the mentioned publications have in common that they were derived for direct current (DC) methods or low-frequency methods, such as time-domain shallow EM methods, or controlled-source EM (CSEM), but not for high-frequency methods such as ground-penetrating radar (GPR). In general, it was even thought that the filter method works only in the diffusive limit where the quasistatic approximation is valid (e.g., Hunziker et al., 2015). Nevertheless, Werthmüller (2017) tests DLF for modeling 250 MHz center-frequency GPR data using a 401 pt filter that was designed for diffusive EM, and found that it was orders of magnitude faster than quadrature approaches. However, good-quality results were only obtained for the first arrivals at short-time offsets and the later arrivals had poor quality. Yet, this promising initial test suggests that it might be possible to specifically design a special filter for GPR frequencies in which the EM fields propagate as waves rather than by diffusion.

Although there are several versions of digital filters that are freely available, there are no open-source filter designing tools that are readily available; they are either only described methods in papers, or the codes are only available upon request by the author. Here, we address this gap by presenting the code `fdesign`, which is an open-source tool for designing general or purpose-built filters using the direct matrix inversion method. The code is completely open

source and can be run using freely available programming environments; thus, there are few barriers to obtaining and running the code.

In the following sections, we give a brief overview of the methodology, the theory, and the code, and then we show examples of its usage, as well as presenting new filters for CSEM and GPR data. Therefore, the current paper falls into all three mentioned categories by the new application of DLF to wave phenomena, which means that the DLF can probably be used to model seismic wavefields as well, and by providing new filters with the accompanying code. The algorithm and many more examples of its use can be found on github.com/empymod/article-fdesign. The examples can be used as templates to design new filters.

METHODOLOGY

The algorithm `fdesign` is a filter designing tool using the direct matrix inversion method as described by Kong (2007) and based on scripts developed by Key (2012). The tool is an add-on to the EM modeler `empymod` (Werthmüller 2017), written in Python and hosted on GitHub, which should foster interaction and enable anyone to toy around, improve, and extend it. It can be used to derive DLFs for the Hankel and the Fourier transforms for potential, diffusive, and wavefield modeling (hence from DC to GPR).

Theoretically, it can be used to derive linear filters for any linear transform, as long as it is supplied with the inputs and outputs of a transform pair. Previous works have relied on using theoretical transform pairs commonly found in tables of integral transforms. Here, we follow a similar approach, but we also propose a new method in which filters can be derived from accurately computed numerical transform pairs, such as those computed using quadrature approaches. For example, the EM modeler `empymod` can be used to compute transform pairs for a particular class of model and data parameters (e.g., a specific EM method and model of interest) using a slow but highly accurate quadrature method. A good filter derived from the resulting transform pairs could then be used for faster modeling of similar model and data parameters.

The main features of `fdesign` and some differences between it and the methods it is based upon are

- The algorithm computes many different filters for various spacing and shift values (brute force), with an optional minimization routine for the best outcome of the brute-force step.
- Kong (2007) and Key (2012) optimize a filter for the J_0 filter, and then they use the obtained shift and spacing value to calculate the J_1 values. The presented algorithm can optimize either J_0, J_1, or both in the optimization process. Five transform pairs for each J_0 and J_1 and three transform pairs for each sine and cosine of often-used functions are included in the routine, but any other transform pair can be provided as input.
- More complex or more specific numerical transform pairs can be provided instead of theoretical transform pairs by using the modeler `empymod`.
- Kong (2007) defines a *good* filter as one that recovers *weak* diffusive EM fields. In `fdesign`, you can define a relative error level that defines up to what error an obtained result is good or not. The optimization seeks to find the smallest amplitude field that is accurately modeled (i.e., minimizing the amplitude), but it has additionally another mode, in which it will maximize the output abscissae r of the transform pair instead of minimizing the amplitude. The two modes yield the same result in the general, simple case of fast-decaying transform pairs. However, for some complex models and specifically for very high frequencies, maximizing r will yield much better and more consistent results.
- The algorithm can solve equal- and over-determined linear systems.
- The real or the imaginary part can be used for the inversion of complex transform pairs.

The quality of a filter depends heavily on the model chosen for comparison. An obtained filter might be very good for one model or data acquisition setup, but not that good for another one, which is no different for this designing tool. There is no way to estimate the error of a result obtained with a certain filter if you apply it to any other model, unless you calculate this other model with another method for comparison. All results presented here should therefore be taken with certain care. Furthermore, when applying a new filter to a significantly different model or data space than what it has previously been tested on, we recommend first verifying its accuracy in that space by a comparison with results computed with a quadrature method such as QWE, which is also available in `empymod`.

Theory

Most of the papers mentioned in the review have detailed derivations of the digital filter method. In this paper, we focus on the algorithm, and we summarize the theory only very briefly by following Key (2012). In EM, we often have to evaluate integrals of the form

$$F(r) = \int_0^\infty f(l)K(lr)\mathrm{d}l, \tag{1}$$

where l and r denote the input and output evaluation values, respectively, and K is the kernel function. In the specific case of the Hankel transform, l corresponds to wavenumber, r to offset, and K to Bessel functions; in the case of the Fourier transform, l corresponds to frequency, r to time, and K to sine or cosine functions. In both cases, it is an infinite integral which numerical integration is very time consuming because of the slow decay of the kernel function and its oscillatory behavior.

By substituting $r = e^x$ and $l = e^{-y}$, we get

$$e^x F(e^x) = \int_{-\infty}^\infty f(e^{-y})K(e^{x-y})e^{x-y}\mathrm{d}y. \tag{2}$$

This can be rewritten as a convolution integral and be approximated for an N-point filter by

$$F(r) \approx \sum_{n=1}^{N} \frac{f(b_n/r)h_n}{r}, \tag{3}$$

where h is the DLF, and the logarithmically spaced filter abscissae is a function of the spacing Δ and the shift δ,

$$b_n = \exp\{\Delta(-\lfloor (N+1)/2 \rfloor + n) + \delta\}. \tag{4}$$

From equation 3, it can be seen that the filter method requires N evaluations at each r. For example, to calculate the frequency-

domain result for 100 offsets with a 201 pt filter requires 20,100 evaluations in the wavenumber domain. This is why the DLF often uses interpolation to minimize the required evaluations, either for $F(r)$ in what is referred to as *lagged convolution DLF*, or for $f(l)$, which we here call *splined DLF*.

In the direct matrix inversion method for solving for the digital filter coefficients, equation 3 is cast as a linear system, where Δ and δ are preassigned scalar values and r is a range of M preassigned values r_m. The filter base coefficients b_n are computed using equation 4 and an array of values for l are computed using $l_{mn} = b_n/r_m$. The linear system's left-hand-side (LHS) matrix $\mathbf{A}$ has dimensions $M \times N$ with coefficients $A_{mn} = f(l_{mn})/r_m$ and the right-hand-side (RHS) vector $\mathbf{v}$ has elements $v_m = F(r_m)$. The resulting linear system

$$\mathbf{Ah} = \mathbf{v} \tag{5}$$

can be solved by direct matrix inversion, or any other matrix inversion routine, to obtain the vector of filter coefficients $\mathbf{h}$. For a given filter length N, there are many subjective choices that go into the practical implementation of this method, including the choice of the transform pairs $F(r)$ and $f(l)$, as well as the value for M and the particular range and spacing of the values r_m. Once values are chosen for these variables, an optimal filter can be found by a grid search over Δ and δ for values that produce a high-quality filter. The choice of metric for what constitutes a high-quality filter is also subjective and is further discussed below.

Pseudocode for fdesign

The main input variables are the filter length (N), the spacing (Δ), and the shift (δ) ranges over which to loop, and the transform pairs for the inversion (f_I) and the check of quality (f_C). If f_C is not provided, then f_I is used for both. There are additional, optional input parameters, for instance, to adjust how the RHS abscissae for the inversion $r_\mathrm{I} = p(b, N)$ are calculated, where b is the filter base. In addition, ranges r for evaluating the check function need to be specified.

The basic steps are as follows:

1) Evaluate the RHS of check function f_C:

$$d_\mathrm{R} = f_\mathrm{C}^\mathrm{RHS}(r).$$

2) Loop over each value Δ_i, δ_j (brute force; parameters on the left side of the equations are overwritten where i, j are not mentioned):

   a) Calculate the filter base:

$$b_n = \exp\{\Delta_i(-\lfloor (N+1)/2 \rfloor + n) + \delta_j\}.$$

   b) Get the required RHS and LHS evaluation points:

$$r_\mathrm{I} = p(b, N)$$

$$l_\mathrm{I} = b/r_\mathrm{I}.$$

   c) Invert for the filter coefficients:

$$J = \mathrm{solve}[f_\mathrm{I}^\mathrm{LHS}(l_\mathrm{I}), f_\mathrm{I}^\mathrm{RHS}(r_\mathrm{I})].$$

   d) Calculate numerically the RHS of check function f_C with current filter J:

$$d_\mathrm{F} = f_\mathrm{C}^\mathrm{LHS}(b/r) \cdot J/r.$$

   e) Store the minimum recovered amplitude or maximum r where the relative error is less than the provided error:

$$\chi_{ij} = g[\mathrm{argmin}(|(d_\mathrm{F} - d_\mathrm{R})/d_\mathrm{R}| > \mathrm{error}) - 1],$$

   where g is either d_R or $1/r$.

3) Recalculate (steps 2a–2c) the filter base and coefficients that yield the minimum amplitude or maximum r (a local minimization can be run to polish the brute-force result):

$$i_\mathrm{best}, j_\mathrm{best} = \mathrm{argmin}(\chi).$$

   Recalculate b, J with i_best, j_best.

4) Return filter base and coefficients and error matrix (for visual QC):
   return b, J, χ.

To solve step 2c, we implemented the QR-decomposition method in `fdesign`.

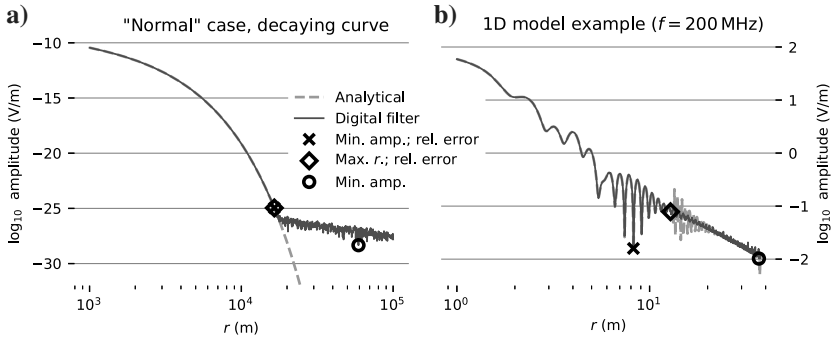

Figure 1. (a) A regular RHS curve of a transform pair with a purely decaying function. The minimum amplitude or maximum r yield the same result in this scenario. Using a relative error criteria is more stable than just the absolute minimum amplitude. (b) A 1D model for $f = 200$ MHz. Here, the maximum r provides better criteria for the inversion.

Minimization criteria

Figure 1 shows the differences between the different minimization approaches: Figure 1a for a conventional, fast decaying transform pair (using the J_0 kernel of a full space with a vertical distance between the source and receiver of 50 m, frequency $f = 1$ Hz, and resistivity $\rho = 1$ Ωm); and Figure 1b for a more complex, high-frequency layered model (using the J_0 kernel for $f = 200$ MHz for the GPR model described in the "Ground-penetrating radar" section, with the receiver located at 1 m depth). The circles show the minimum amplitude used in previous approaches. This criterion is not ideal

because it is subject to some random fluctuations and it depends on the choice of r. The squares show the minimum amplitude given a certain acceptable error, and the diamonds show the maximum r given a certain acceptable error (the inversion is a minimization process; therefore, it minimizes $1/r$, not r). In simple cases, the minimum amplitude given an acceptable error and the maximum r given an acceptable error will yield the same result. However, in complex cases, the maximum r is more consistent and is therefore a much better criterion.

Although the χ array is used to identify the optimal values of Δ and δ, the value of $\mathrm{argmin}(\chi)$ will depend on the choice of the check function f_C and can vary from one transform pair to another; thus, it should not be used to compare the quality of filters created with different transform pairs.

NUMERICAL EXAMPLES

The numerical examples are focused on the Hankel transform, although `fdesign` can be used to design DLFs for the Hankel and Fourier transforms. Because there is no difference in the procedure of the two, this should be sufficient to demonstrate the algorithm.

Design

Figures 2 and 3 show the solution spaces of seven consecutive inversion runs using the following theoretical transform pairs (e.g., Anderson, 1975):

$$\int_0^\infty l\exp(-al^2)J_0(rl)dl = \frac{1}{2a}\exp\left(\frac{-r^2}{4a}\right), \qquad (6)$$

$$\int_0^\infty l^2\exp(-al^2)J_1(rl)dl = \frac{r}{4a^2}\exp\left(-\frac{r^2}{4a}\right), \qquad (7)$$

where a was set to five. In the algorithm, you can provide one pair for the inversion, and a different pair to get the minimum amplitude or the maximum r. In this case, the same transform pair was used for the inversion and the check of quality. The acceptable relative error was set to 1%. The RHS evaluation parameter for the inversion was set so that an over-determined system was evaluated with $M = 2N$ equations, where r_I was logarithmically spaced from $\log_{10}[1/\max(b)] - 1$ to $\log_{10}[1/\min(b)] + 1$, where b are the filter abscissae as given in equation 4. This is accomplished in `fdesign` by setting parameter $r_\mathrm{def} = (1, 1, 2)$.

Figure 2 shows three different inversion runs for $N = 101$, 201, and 401 for a wide range of spacing and shift values. From this, one has to decide on a filter length. Longer filters tend to give more precise results, but their transform is computationally more expensive because more values have to be evaluated. The length of the filter does not have to be an odd number, but many published filters do have an odd number of coefficients. The integral runs from $-\infty$ to $+\infty$; hence, an odd point filter comes naturally by truncating the integral to a finite sum from $-(N-1)/2$ to $(N-1)/2$. However, this is only true if the shift value $\delta = 0$. If it differs from zero, then there is no advantage in having an odd point filter.

Figure 3 shows four consecutive inversion runs for $N = 201$, where each run is a focus on a subsection of the previous run, indicated by the square. From the low-resolution overview runs in Figures 2, 3a and 3b, it looks like this is a standard, straightforward minimization problem. However, from the more detailed results in Figure 3c and 3d, it becomes obvious that it is a minimization problem that has to be solved stochastically because there are solutions with two orders of magnitude difference apparently randomly next to each other.

Figure 4a shows the filter values for J_0 and J_1 of the best 201 pt filter obtained this way, and Figure 4b shows its RHS solution. The black dots indicate negative values, from which it can be seen that adjacent values are often alternating between positive and negative contributions.

Designing filters is to a large extent trial and error. All input variables influence the outcome, and often an even better filter is found by sheer luck of choosing the right starting parameters, as can be seen in Figure 3d. However, once you are in this zone, every filter is a very good filter. Each of the input parameters has an effect on the outcome. It also depends on the transform pairs $f_\mathrm{I;C}$; functions that decay rapidly are generally better, as noted by earlier authors (e.g., Anderson, 1975). Other important factors are the filter length and the spacing and shift values, as well as how you define the right-hand evaluation points of the inversion (r_def). Evaluating

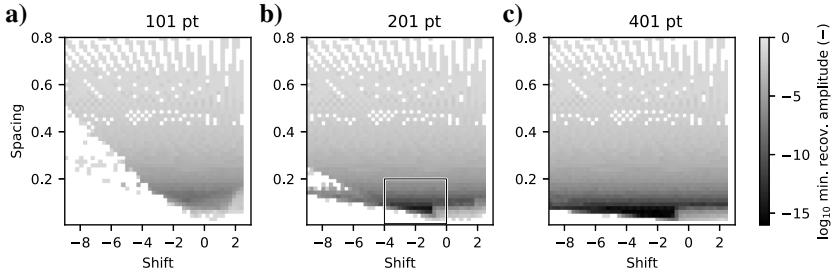

Figure 2. Test of different filter lengths. The filter length is a trade-off between precision and speed because shorter filters are faster but less precise and longer filters are more precise but computationally more expensive. The square in (b) is the starting point of Figure 3.

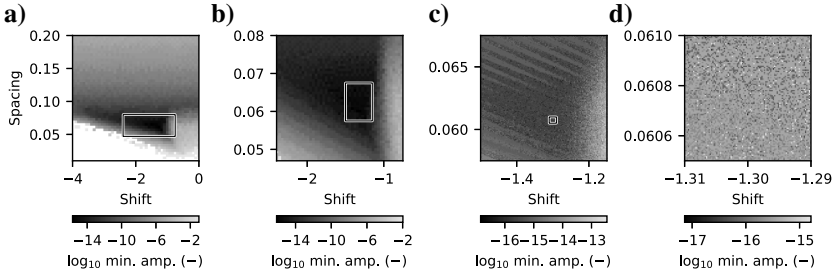

Figure 3. Solution spaces of four consecutive inversion runs for a 201 pt filter. Each consecutive run magnifies into a portion of the previous solution space, indicated by the square. The more in detail we obtain the solution space, the more random the distribution appears to be.

corresponding transform pairs separately or jointly also leads to different filter coefficients (J_0, J_1, or J_0 and J_1, or equally sine, cosine, or sine and cosine); also if the real or the imaginary part is used when complex transform pairs or `empymod` is used; and if it is inverted for the minimum amplitude or for the maximum r.

CSEM

In this section, we compare the 201 pt filter derived in the previous section to marine CSEM models as used in Kong (2007), Key (2012), and for a land EM case.

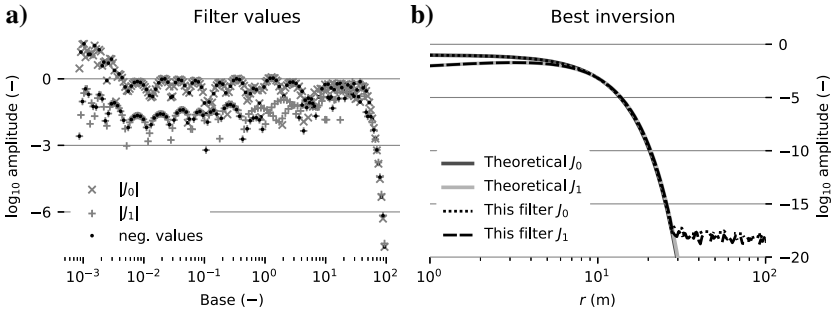

Figure 4. (a) Filter values of the best obtained 201 pt filter with the corresponding check of quality in (b). The black points indicate negative values, which show that adjacent values have often opposite signs.

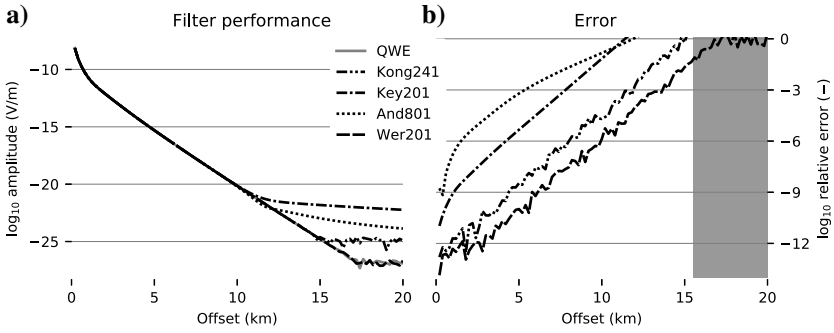

Figure 5. (a) Results of different filters and QWE for the model of Figure 5 from Kong (2007) with the relative errors shown in (b), using the QWE result. The relative error is meaningless from approximately 15.5 km onward because QWE failed as well for these very low amplitudes.

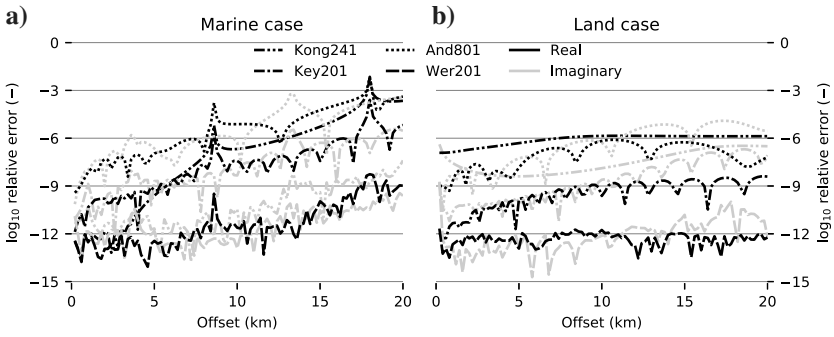

Figure 6. (a) The canonical marine CSEM model of Key (2012) and (b) a land model with the source and receiver at the surface. The new filter shows relative errors that are generally several orders of magnitude lower than for the other filters.

Figure 5 compares the derived 201 pt filter with the two half-spaces case used by Kong (2007) in his Figure 5. The model consists of a 0.3125 Ωm sea layer of infinite thickness above a subsurface half-space of 1 Ωm. The signal of a 1 Hz x-directed electric source 50 m above the interface is measured at an x-directed electric receiver at the interface. In Figure 5a, it can be seen that the new 201 pt filter is able to recover smaller amplitudes than the 241 pt filter from Kong (2007), the 201 pt filter from Key (2012), and the 801 pt filter from Anderson (1982) (Wer201, Kong241, Key201, and And801, respectively). It behaves equally well as the QWE, for which we used a 51 pt quadrature with relative and absolute tolerance of 10^{-12} and 10^{-30}, respectively. The relative error is shown in Figure 5b, in which the QWE result was taken as *truth*. For offsets greater than approximately 15.5 km, the relative error becomes meaningless because the QWE fails itself; this part is grayed out in Figure 5.

Figure 6a considers the canonical CSEM model as used by Key (2012) in his Figure 5: a 0.303 Ωm sea with depth of 2 km, a background resistivity of 1 Ωm, in which a 100 Ωm target layer of 100 m thickness is embedded at 1 km below the seafloor. The source is located at 1990 m, and receivers are positioned on the seafloor.

Figure 6b is a land case, with a background resistivity of 10 Ωm, in which a 500 Ωm target of 100 m thickness is embedded at 1 km below the surface. The source depth is 0.5 m, and the receiver depth is 0.8 m. In both cases, the new filter Wer201 generally has a relative error that is orders of magnitude lower than the other filters. The relative error of the real part is given in black, whereas the relative error of the imaginary part is given in gray. It is interesting to note that the real and imaginary parts have very similar errors in Wer201, Key201, and And801, but that the imaginary part of Kong241 seems to behave considerably better for most part than its real counterpart. To compare the real and the imaginary parts is insofar interesting because the digital filters are purely real valued.

It is very important to note again that other scenarios might yield very different error plots. Although the new 201 pt filter proves to be very accurate for these three models, it might not be the best filter in other cases. To verify the applicability of the filter, we run two different tests over a wide range of scenarios. Figure 7 shows the relative errors of DLF using the filter Wer201 compared with QWE for a deepwater model (2 km water depth), a shallow-water model (400 m water depth), and a land model. The models consist of air (upper half-space), a water layer in the first two examples, and a subsurface half-space. The source depth is 1990, 10, and 0.5 m in the deep, shallow, and land cases, respectively. The receiver depth is 2000, 100, and 0.8 m. The subsurface half-space resistivity varies from

1 to 10, 100, and 1000 Ωm from the left to the right column. The error plots cover offsets from 50 m to 20 km on the x-axis and 0.01 to 10 Hz on the y-axis. It can be seen in the result that the filter is sufficiently precise for all practical CSEM cases; hence, it generally has an error far below 1% (10^{-2}) in all cases. A relative noise of less than 1% is generally considered really good for real data. The exceptions are in the shallow-water case at large offsets with relatively high frequencies, e.g., 10 km offset with 8 Hz; this zone has a very high error for subsurface resistivities of 1 and 10 Ωm (the yellow zones). However, this is due to the fact that the amplitudes of the signal for these offsets and frequencies are in the order of 10^{-25} V/m. The gray contour lines in the plot indicate the logarithm of the signal amplitude.

Another error test is shown in Figure 8. Figure 8a shows the amplitude of the analytical fullspace solution for a wide range of resistivities and frequencies: $\rho = 10^{-10}$ to 10^{10} Ωm, and $f = 10^{-10}$ to 10^{14} Hz. In this case, the horizontal offset is set to the skin depth, and the vertical source-receiver separation to a tenth of it, where the skin depth is given by Ward and Hohmann, 1988 (equation 1.49)

$$z_{\text{skin}} = \left\{ \frac{\omega^2 \varepsilon \mu}{2} \left[\sqrt{1 + \frac{1}{(\omega \varepsilon \rho)^2}} - 1 \right] \right\}^{-1/2}, \tag{8}$$

where we used in the example $10\varepsilon_0$ for the electric permittivity and μ_0 for the magnetic permeability; $\omega = 2\pi f$. The gray contour lines in Figure 8 show the $\log_{10}$ scaled magnitude of the offset: the line with zero where the offset is 1 m, the line with three where the offset is 1 km, etc. The contour lines of the offset have a knee, after which they become almost independent of frequency. This is where the quasistatic approximation breaks down and wave phenomena become dominant. The red line indicates where $\omega\varepsilon\rho = 1$. Figure 8b shows the relative error of the DLF using the filter Wer201 compared with the analytical solution. It nicely shows that the filter can be used for all cases that are in the quasistatic region, but not outside.

We also comment that although it is tempting to design very short length filters (much less than about $N = 100$) because shorter filters can greatly reduce EM simulation times, in our experience, shorter filters tend to be less general purpose than longer filters and we highly recommend thoroughly testing their accuracy for the desired range of data and model parameters.

GPR

Figure 9 shows the GPR example as calculated by Hunziker et al. (2015) and Werthmüller (2017), and the model parameters are given in Figure 9a. The filter used for this example for the Hankel transform is a 2001 pt filter, derived with the full-space solution with $f = 500$ MHz for the inversion and the check of quality. The whole-space solution used resistivity of 200 Ωm, relative permittivity of $\varepsilon_r = 10$, and permeability of $\mu_r = 1$. Using equation 8 yields a skin depth of approximately 3.6 m for these parameters. The source and receiver vertical separation is 1 m. For the Fourier transform, a 4096 pt FFT was used with regularly spaced frequencies from 0.5 to 850 MHz and then zero-padded up to 2048 MHz. The frequency result is multiplied with a Ricker wavelet

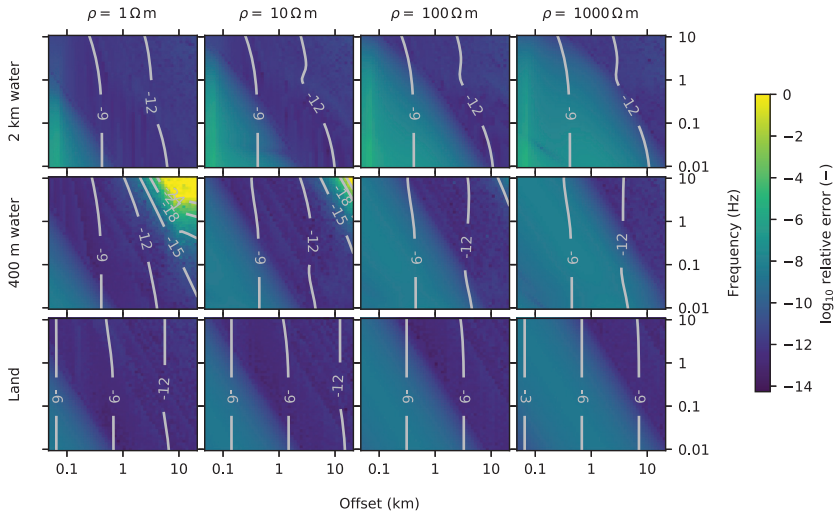

Figure 7. Relative error plots comparing the DLF (Wer201) with QWE for the three cases: deep water (top row), shallow water (middle row), and land (bottom row). The subsurface half-space resistivity varies from 1 to 1000 Ωm from the left column to the right column; offsets vary from 50 m to 20 km, and frequencies vary from 0.01 to 10 Hz. The DLF provides sufficiently accurate results for all practical CSEM applications. The exception is in the shallow-water case for $\rho = 1$ and 10 Ωm for large offsets and high frequencies (the yellow zones). However, the amplitudes in these regions are in the order of 10^{-25} V/m, and therefore several orders of magnitude below the noise levels of current EM instrument systems. Contour lines show the corresponding $\log_{10}$ scaled signal amplitudes.

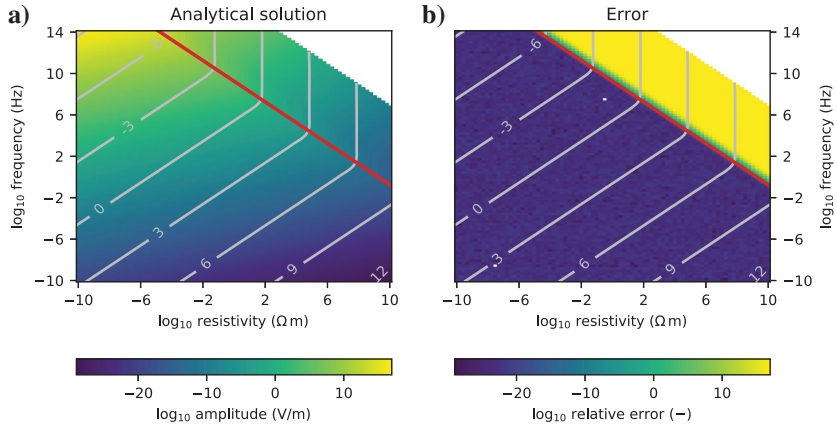

Figure 8. (a) Amplitude of the analytical full-space solution for a wide range of resistivities and frequencies. The contour lines show the $\log_{10}$ scaled offset used for the calculation, where the offset is set to the skin depth. (b) Relative error of the DLF compared with the analytical solution. The filter Wer201 works well in the diffusive limit, but fails when wave phenomena become dominant. The red line shows where $\omega\varepsilon\rho = 1$.

with a center frequency of 250 MHz, and a gain function ($1 + |t^3|, t$ in ns) is applied. Figure 9b shows the result when using the adaptive quadrature (QUAD) option of `empymod`, which uses the QAGSE routine from the Fortran QUADPACK library. Figure 9c shows the result using DLF with the new 2001 pt digital filter. The calculation with DLF took less than 9 min and is therefore approximately 80 times faster than the calculation with QUAD, which took approximately 11 h and 27 min. Calculating the same model with QWE took 7 h and 20 min. However, QWE uses approximately one-third of the calculation internally QUAD in this example, see Werthmüller (2017). Note that DLF was run in parallel using four threads at once, taking effectively only 2 min and 10 s to calculate. The lagged convolution version of DLF and the splined version of QWE were used in this comparison.

Figure 10a–10c shows the real and imaginary parts of the frequency-domain results, and Figure 10d–10f shows the time-domain results for offsets of 0.2, 2.0, and 3.0 m.

The 2001 pt filter was derived with the full-space solution of a medium, which is very similar to the layer in which the source and receiver reside in our GPR example. To show that this filter can also be applied to different layer parameters, we run a test in which we swapped layers one and two of the model in Figure 9a. The resulting real and imaginary parts for the offsets 0.2, 2.0, and 3.0 m are given in Figure 11.

These examples clearly show that the filter method can indeed be applied to high-frequency EM modeling and therefore wave phenomena. We are convinced that with further tests and analysis much better filters could be achieved, and various concepts could be checked. One approach is to derive a filter for each frequency band, say one for 1–10 MHz, one for 10–100 MHz, and one for 100 MHz to 1 GHz. Another approach could be to derive distinct filters for J_0 and J_1, with different spacing and shift values. The first idea would roughly triple the calculation cost, the second idea double them; however, they both would still be very fast compared with standard quadrature methods. One could also apply the digital filter method to acoustic and elastic wavefields as well.

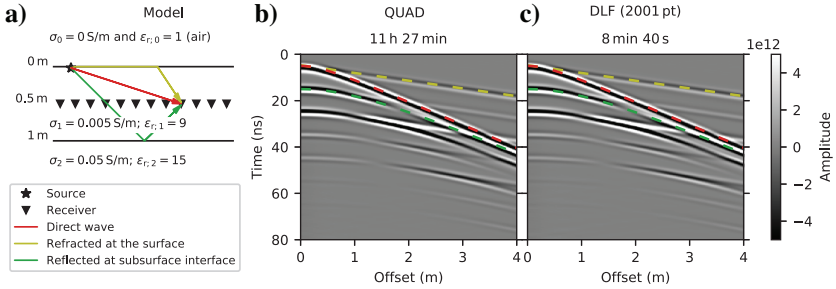

Figure 9. The GPR example for the model given in (a) using `empymod` with (b) adaptive quadrature (QUAD) or with (c) a 2001 pt DLF. QUAD took approximately 11 h 27 min to calculate, whereas DLF took 2 min 10 s in parallel on four nodes, hence under 9 min in total.

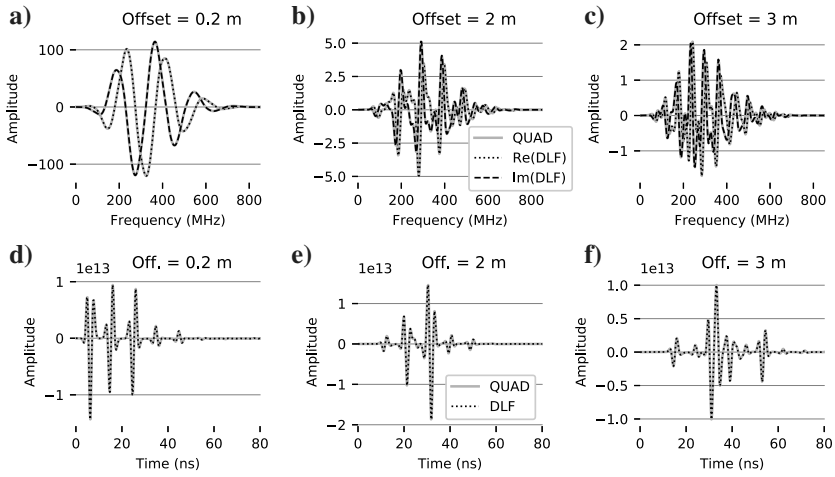

Figure 10. (a-c) The real and imaginary parts of the frequency-domain responses and (d-f) the time-domain responses for horizontal offsets of (a and d) 0.2 m, (b and e) 2.0 m, and (c and f) 3.0 m.

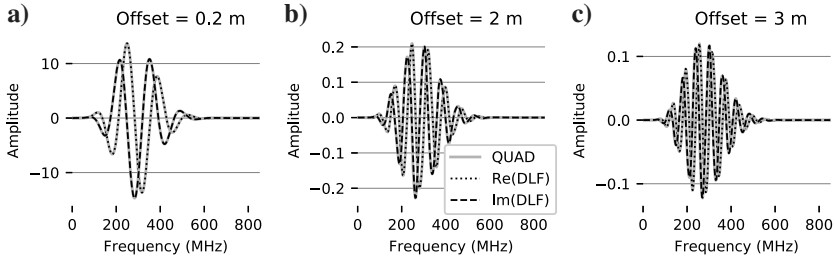

Figure 11. The real and imaginary parts of the frequency-domain response for the model given in Figure 9a with swapped first and second layers for horizontal offsets of (a) 0.2 m, (b) 2.0 m, and (c) 3.0 m.

CONCLUSION

The presented, free, and open-source code `fdesign` can be used to design DLFs for the Hankel and Fourier transforms (and more generally for any linear transform) using either analytical transform pairs or 1D subsurface models together with the EM modeler `empymod`. The code is available from GitHub as part of `empymod`; the version corresponding to this publication is v1.8.1.

The presented 201 pt filter achieves more precise results in the three presented CSEM cases than other filters, and it is included in `empymod` from version 1.4.5 onward. However, as with any digital filter, the quality depends heavily on the model, and this new filter might or might not behave that well for other models or data parameters.

The GPR example shows that the DLF method can also be used for wave phenomena, not only for the diffusive approximation limit of low-frequency EM modeling.

We see `fdesign` as being useful for at least three scenarios:

1) Providing a fast method to design problem-specific filters. For bigger inversion projects (such as, for instance, massive stochastic CSEM inversions), a purpose-designed, short filter might save much more time than it costs to design it. This could even be integrated into inversion codes, as an optional preinversion step.
2) Extending the filter method to new areas, namely, higher frequencies and acoustic and elastic wavefields.
3) Raising interest for DLFs in geophysics by making it very easy for anyone to play around, create their own filters, and get a better understanding of the relative simplicity of the method. We are sure there are many great filters that are yet to be discovered.

ACKNOWLEDGMENTS

D. Werthmüller would like to thank the EM research group of A. Mousatov at the IMP for fruitful discussions, and J. Hunziker for valuable feedback that improved this manuscript considerably. We thank the assistant editor J. Etgen, the associate editor J. Dellinger, and the reviewers C. Weiss and R. Mittet for valuable input not only regarding the manuscript but also regarding the code and its documentation.

DATA AND MATERIALS AVAILABILITY

Data associated with this research are available and can be accessed via the following URL: https://doi.org/10.5281/zenodo.1492840.

REFERENCES

Anderson, W. L., 1973, Fortran IV programs for the determination of the transient tangential electric field and vertical magnetic field about a vertical magnetic dipole for an m-layer stratified earth by numerical integration and digital linear filtering: USGS, PB221240, https://ntrl.ntis.gov/NTRL/dashboard/searchResults/titleDetail/PB221240.xhtml, accessed 25 July 2017.

Anderson, W. L., 1975, Improved digital filters for evaluating Fourier and Hankel transform integrals: USGS, PB242800, https://pubs.er.usgs.gov/publication/70045426, accessed 15 February 2016.

Anderson, W. L., 1979, Numerical integration of related Hankel transforms of orders 0 and 1 by adaptive digital filtering: Geophysics, **44**, 1287–1305, doi: 10.1190/1.1441007.

Anderson, W. L., 1982, Fast Hankel transforms using related and lagged convolutions: ACM Transactions on Mathematical Software, **8**, 344–368, doi: 10.1145/356012.356014.

Anderson, W. L., 1984, On: "Numerical integration of related Hankel transforms by quadrature and continued fraction expansion" by A. D. Chave: Geophysics, **49**, 1811–1812, doi: 10.1190/1.1441595.

Anderson, W. L., 1989, A hybrid fast Hankel transform algorithm for electromagnetic modeling: Geophysics, **54**, 263–266, doi: 10.1190/1.1442650.

Bernabini, M., and E. Cardarelli, 1978, The use of filtered Bessel functions in direct interpretation of geoelectrical soundings: Geophysical Prospecting, **26**, 841–852, doi: 10.1111/j.1365-2478.1978.tb01636.x.

Bichara, M., and J. Lakshmanan, 1976, Fast automatic processing of resistivity soundings: Geophysical Prospecting, **24**, 354–370, doi: 10.1111/j.1365-2478.1976.tb00932.x.

Christensen, N. B., 1990, Optimized fast Hankel transform filters: Geophysical Prospecting, **38**, 545–568, doi: 10.1111/j.1365-2478.1990.tb01861.x.

Das, U. C., 1982, Designing digital linear filters for computing resistivity and electromagnetic sounding curves: Geophysics, **47**, 1456–1459, doi: 10.1190/1.1441295.

Das, U. C., 1984, A single digital linear filter for computations in electrical methods — A unifying approach: Geophysics, **49**, 1115–1118, doi: 10.1190/1.1441726.

Das, U. C., and D. P. Ghosh, 1974, The determination of filter coefficients for the computation of standard curves for dipole resistivity sounding over layered earth by linear digital filtering: Geophysical Prospecting, **22**, 765–780, doi: 10.1111/j.1365-2478.1974.tb00117.x.

Das, U. C., D. P. Ghosh, and D. T. Biewinga, 1974, Transformation of dipole resistivity sounding measurements over layered earth by linear digital filtering: Geophysical Prospecting, **22**, 476–489, doi: 10.1111/j.1365-2478.1974.tb00100.x.

Das, U. C., and S. K. Verma, 1980, Digital linear filter for computing type curves for the two-electrode system of resistivity sounding: Geophysical Prospecting, **28**, 610–619, doi: 10.1111/j.1365-2478.1980.tb01246.x.

Das, U. C., and S. K. Verma, 1981a, Numerical considerations on computing the EM response of three-dimensional inhomogeneities in a layered earth: Geophysical Journal International, **66**, 733–740, doi: 10.1111/j.1365-246X.1981.tb04897.x.

Das, U. C., and S. K. Verma, 1981b, The versatility of digital linear filters used in computing resistivity and EM sounding curves: Geoexploration, **18**, 297–310, doi: 10.1016/0016-7142(81)90059-4.

Das, U. C., and S. K. Verma, 1982, Electromagnetic response of an arbitrarily shaped three-dimensional conductor in a layered earth — Numerical results: Geophysical Journal International, **69**, 55–66, doi: 10.1111/j.1365-246X.1982.tb04935.x.

Davis, P. A., S. A. Greenhalgh, and N. P. Merrick, 1980, Resistivity sounding computations with any array using a single digital filter: Exploration Geophysics, **11**, 54–62, doi: 10.1071/EG980054.

Ghosh, D. P., 1970, The application of linear filter theory to the direct interpretation of geoelectrical resistivity measurements: Ph.D. thesis, Delft University of Technology.

Ghosh, D. P., 1971a, The application of linear filter theory to the direct interpretation of geoelectrical resistivity sounding measurements: Geophysical Prospecting, **19**, 192–217, doi: 10.1111/j.1365-2478.1971.tb00593.x.

Ghosh, D. P., 1971b, Inverse filter coefficients for the computation of apparent resistivity standard curves for a horizontally stratified earth: Geophysical Prospecting, **19**, 769–775, doi: 10.1111/j.1365-2478.1971.tb00915.x.

Guptasarma, D., 1982, Optimization of short digital linear filters for increased accuracy: Geophysical Prospecting, **30**, 501–514, doi: 10.1111/j.1365-2478.1982.tb01320.x.

Guptasarma, D., and B. Singh, 1997, New digital linear filters for Hankel J0 and J1 transforms: Geophysical Prospecting, **45**, 745–762, doi: 10.1046/j.1365-2478.1997.500292.x.

Hunziker, J., J. Thorbecke, and E. Slob, 2015, The electromagnetic response in a layered vertical transverse isotropic medium: A new look at an old problem: Geophysics, **80**, no. 1, F1–F18, doi: 10.1190/geo2013-0411.1.

Johansen, H. K., 1975, An interactive computer/graphic-display-terminal system for interpretation of resistivity soundings: Geophysical Prospecting, **23**, 449–458, doi: 10.1111/j.1365-2478.1975.tb01541.x.

Johansen, H. K., and K. Sørensen, 1979, Fast Hankel transforms: Geophysical Prospecting, **27**, 876–901, doi: 10.1111/j.1365-2478.1979.tb01005.x.

Key, K., 2009, 1D inversion of multicomponent, multifrequency marine CSEM data: Methodology and synthetic studies for resolving thin resistive layers: Geophysics, **74**, no. 2, F9–F20, doi: 10.1190/1.3058434.

Key, K., 2012, Is the fast Hankel transform faster than quadrature?: Geophysics, **77**, no. 3, F21–F30, doi: 10.1190/GEO2011-0237.1.

Koefoed, O., 1968, The application of the kernel function in interpreting geoelectrical resistivity measurements: Gebrüder Borntraeger.

Koefoed, O., 1970, A fast method for determining the layer distribution from the raised kernel function in geoelectrical sounding: Geophysical Prospecting, **18**, 564–570, doi: 10.1111/j.1365-2478.1970.tb02129.x.

Koefoed, O., 1972, A note on the linear filter method of interpreting resistivity sounding data: Geophysical Prospecting, **20**, 403–405, doi: 10.1111/j.1365-2478.1972.tb00643.x.

Koefoed, O., 1976, Error propagation and uncertainty in the interpretation of resistivity sounding data: Geophysical Prospecting, **24**, 31–48, doi: 10.1111/j.1365-2478.1976.tb00383.x.

Koefoed, O., and F. J. H. Dirks, 1979, Determination of resistivity sounding filters by the Wiener-Hopf least-squares method: Geophysical Prospecting, **27**, 245–250, doi: 10.1111/j.1365-2478.1979.tb00968.x.

Koefoed, O., D. P. Ghosh, and G. J. Polman, 1972, Computation of type curves for electromagnetic depth sounding with a horizontal transmitting coil by means of a digital linear filter: Geophysical Prospecting, **20**, 406–420, doi: 10.1111/j.1365-2478.1972.tb00644.x.

Kong, F. N., 2007, Hankel transform filters for dipole antenna radiation in a conductive medium: Geophysical Prospecting, **55**, 83–89, doi: 10.1111/j.1365-2478.2006.00585.x.

Kruglyakov, M., and L. Bloshanskaya, 2017, High-performance parallel solver for integral equations of electromagnetics based on Galerkin method: Mathematical Geosciences, **49**, 751–776, doi: 10.1007/s11004-017-9677-y.

Kumar, R., and U. C. Das, 1977, Transformation of dipole to Schlumberger sounding curves by means of digital linear filters: Geophysical Prospecting, **25**, 780–789, doi: 10.1111/j.1365-2478.1977.tb01204.x.

Kumar, R., and U. C. Das, 1978, Transformation of Schlumberger apparent resistivity to dipole apparent resistivity over layered earth by the application of digital linear filters: Geophysical Prospecting, **26**, 352–358, doi: 10.1111/j.1365-2478.1978.tb01598.x.
Mohsen, A. A., and E. A. Hashish, 1994, The fast Hankel transform: Geophysical Prospecting, **42**, 131–139, doi: 10.1111/j.1365-2478.1994.tb00202.x.
Murakami, Y., and T. Uchida, 1982, Accuracy of the linear filter coefficients determined by the iteration of the least-squares method: Geophysics, **47**, 244–256, doi: 10.1190/1.1441331.
Newman, G. A., G. W. Hohmann, and W. L. Anderson, 1986, Transient electromagnetic response of a three-dimensional body in a layered earth: Geophysics, **51**, 1608–1627, doi: 10.1190/1.1442212.
Nissen, J., and T. Enmark, 1986, An optimized digital filter for the Fourier transform: Geophysical Prospecting, **34**, 897–903, doi: 10.1111/j.1365-2478.1986.tb00500.x.
Niwas, S., 1975, Direct interpretation of geoelectric measurements by the use of linear filter theory: Geophysics, **40**, 121–122, doi: 10.1190/1.1440510.
Nyman, D. C., and M. Landisman, 1977, VES dipole-dipole filter coefficients: Geophysics, **42**, 1037–1044, doi: 10.1190/1.1440763.
O'Neill, D., 1975, Improved linear filter coefficients for application in apparent resistivity computations: Exploration Geophysics, **6**, 104–109, doi: 10.1071/EG975104.
O'Neill, D. J., and N. P. Merrick, 1984, A digital linear filter for resistivity sounding with a generalized electrode array: Geophysical Prospecting, **32**, 105–123, doi: 10.1111/j.1365-2478.1984.tb00720.x.
Pekeris, C. L., 1940, Direct method of interpretation in resistivity prospecting: Geophysics, **5**, 31–42, doi: 10.1190/1.1441791.
Raiche, A., F. Sugeng, and G. Wilson, 2007, Practical 3D EM inversion — The P223F software suite: ASEG Technical Program Expanded Abstracts, 1–4, doi: 10.1071/ASEG2007ab114.
Slichter, L. B., 1933, The interpretation of the resistivity prospecting method for horizontal structures: Physics, **4**, 307–322, doi: 10.1063/1.1745198.
Sørensen, K. I., and N. B. Christensen, 1994, The fields from a finite electrical dipole — A new computational approach: Geophysics, **59**, 864–880, doi: 10.1190/1.1443646.
Verma, R. K., and O. Koefoed, 1973, A note on the linear filter method of computing electromagnetic sounding curves: Geophysical Prospecting, **21**, 70–76, doi: 10.1111/j.1365-2478.1973.tb00015.x.
Ward, S. H., and G. W. Hohmann, 1988, Electromagnetic theory for geophysical applications: SEG, Investigations in Geophysics 4, 130–131.
Werthmüller, D., 2017, An open-source full 3D electromagnetic modeler for 1D VTI media in Python: empymod: Geophysics, **82**, no. 6, WB9, doi: 10.1190/geo2016-0626.1.